Cross-Bridge Attachment during High-Speed Active Shortening of Skinned Fibers of the Rabbit Psoas Muscle: Implications for Cross-Bridge Action during Maximum Velocity of Filament Sliding

R. Stehle and B. Brenner
Molekular- und Zellphysiologie, Medizinische Hochschule Hannover, D-30625 Hannover, Germany

ABSTRACT To characterize the kinetics of cross-bridge attachment to actin during unloaded contraction (maximum velocity of filament sliding), ramp-shaped stretches with different stretch-velocities (2–40,000 nm per half-sarcomere per s) were applied to actively contracting skinned fibers of the rabbit psoas muscle. Apparent fiber stiffness observed during such stretches was plotted versus the speed of the imposed stretch (stiffness-speed relation) to derive the rate constants for cross-bridge dissociation from actin. The stiffness-speed relation obtained for unloaded shortening conditions was shifted by about two orders of magnitude to faster stretch velocities compared to isometric conditions and was almost identical to the stiffness-speed relation observed in the presence of MgATPγS at high Ca^{2+} concentrations, i.e., under conditions where cross-bridges are weakly attached to the fully Ca^{2+} activated thin filaments. These data together with several control experiments suggest that, in contrast to previous assumptions, most of the fiber stiffness observed during high-speed shortening results from weak cross-bridge attachment to actin. The fraction of strongly attached cross-bridges during unloaded shortening appears to be as low as some 1–5% of the fraction present during isometric contraction. This is about an order of magnitude less than previous estimates in which contribution of weak cross-bridge attachment to observed fiber stiffness was not considered. Our findings imply that 1) the interaction distance of strongly attached cross-bridges during high-speed shortening is well within the range consistent with conventional cross-bridge models, i.e., that no repetitive power strokes need to be assumed, and 2) that a significant part of the negative forces that limit the maximum speed of filament sliding might originate from weak cross-bridge interactions with actin.

INTRODUCTION

It is widely accepted that muscle contraction is driven by the interaction of the myosin head domain, forming cross-bridges, with the thin, actin-containing filaments. This interaction is driven by the hydrolysis of MgATP, presumably of one MgATP molecule per myosin head per cycle (A. F. Huxley, 1957; H. E. Huxley, 1969; Lymn and Taylor, 1971; Huxley and Simmons, 1971, 1973; Adelstein and Eisenberg, 1980; Eisenberg et al., 1980; Eisenberg and Hill, 1985). Based on studies in solution and on skinned fibers it was proposed that during this ATPase cycle cross-bridges alternate between two groups of states, the group of weakly binding states and the group of strongly binding cross-bridge states (Eisenberg and Greene, 1980; Rosenfeld and Taylor, 1984; Eisenberg and Hill, 1985; Brenner 1990; Rayment et al., 1993). According to this model it is thought that strongly attached cross-bridges include the main force-generating states; i.e., weakly attached cross-bridges make little if any contribution to active force because they would rapidly detach if strained (cf. Hill, 1974). While it is widely accepted that filament sliding is driven by force-generating, strongly attached cross-bridges, some of the kinetics of cross-bridge action and their correlation with the ATPase pathway are still unclear for some features, even on a merely qualitative basis. For instance, even the basic features of active cross-bridge turnover during high-speed shortening are still unclear. As a consequence, the question was raised whether during high-speed shortening a cross-bridge can remain attached to one and the same actin monomer while passing through the strongly binding states of its cycle, a central assumption of all conventional cross-bridge models (e.g., A.F. Huxley, 1957; Eisenberg and Hill, 1978; Eisenberg et al., 1980; Eisenberg and Greene, 1980; Siemanowskyet al., 1985; Pate et al., 1993). This issue was raised when isotonic fiber ATPase, used as a measure for the cross-bridge cycling time, was compared with isotonic fiber stiffness, used to estimate the fraction of the cycling time during which cross-bridges are strongly attached to actin (duty ratio; cf. Burton, 1992, for a review). For maximum unloaded shortening at v_{max}, this comparison implied that, while cross-bridges pass through the strongly binding states, actin and myosin filaments slide past each other over a distance (the "interaction distance"; cf. Burton, 1992) that is very much longer than the size of a cross-bridge (Higuchi and Goldmann, 1991, 1995; Burton, 1992). It was therefore proposed that, in contrast to conventional models, cross-bridges do not stay attached to the same binding site on actin while passing through strongly binding states. Instead, several mechanisms were proposed that might allow for the interaction of cross-bridges with several sites on an actin filament during passing the strongly attached states of the ATPase cycle (e.g., Brenner, 1991; Piazzesi et al., 1992; Lombardi et al., 1992; Cooke et al., 1994; Piazzesi and

Received for publication 30 July 1999 and in final form 13 December 1999.
Address reprint requests to Dr. R. Stehle, Institut für Vegetative Physiologie, Universität Köln, Robert Koch Strasse 39, D-50931 Köln, Germany. Tel. +49-221-4786952; Fax: +49-221-4786965; E-mail: robert.stehle@uni-koeln.de.

0006-3495/00/03/1458/16 $2.00

Lombardi, 1995). One critical point in arriving at such long interaction distances during high-speed shortening, however, is the assumption that only cross-bridges in strongly binding states contribute to the observed fiber stiffness. Here we report an investigation that was aimed at characterizing actin-binding kinetics of cross-bridges during isometric and unloaded isotonic contraction to test whether, in contrast to previous assumptions, weak cross-bridge attachment to actin could make a significant contribution to fiber stiffness specifically during high-speed shortening. This study was initiated by the observation that myosin heads in weakly binding states, generated in the presence of MgATPγS, showed much slower kinetics for dissociation from and rebinding to actin at saturating Ca^{2+} concentration than seen in the absence of Ca^{2+} (Kraft et al., 1992), although there was little if any effect of Ca^{2+} on actin affinity of these cross-bridge states. This opened the possibility that weak cross-bridge interaction with actin might make a quite substantial contribution to stiffness measurements in activated fibers if Ca^{2+} has a similar effect on actin-binding kinetics of the weakly binding intermediates present during active turnover. In addition, a preliminary evaluation of cross-bridge turnover kinetics for isotonic contraction of skinned fibers from fiber ATPase and transient kinetics observed upon changeover to isovelocity contraction (Brenner, 1988a; Brenner and Stehle, 1994) also suggested that during high-speed shortening only a very small fraction of cross-bridges occupy strongly binding states, in agreement with recent biochemical studies of freely shortening myofibrils (Ma and Taylor, 1994; Lionne et al., 1995).

Using stiffness-speed relations to characterize actin-binding kinetics of cross-bridges (cf. Schoenberg et al., 1984; Schoenberg, 1985, 1988; Brenner et al., 1986a; Brenner, 1990), we found that actin-binding kinetics of the cross-bridge population present during high-speed shortening are very similar to those found in the presence of the ATP analog MgATPγS at saturating Ca^{2+} concentration. This is consistent with the concept that during high-speed shortening the majority of cross-bridges are not strongly attached to actin but rather occupy weakly binding cross-bridge states. Estimates of the fraction of strongly attached cross-bridges for unloaded shortening suggest a rather low value of some 1–5% of the fraction of strongly attached during isometric steady-state contraction. This value is about an order of magnitude lower than previously derived from total stiffness with the tacit assumption that the contribution of weakly attached cross-bridges to isotonic fiber stiffness can be neglected (Burton, 1992). Estimates of the interaction distance during high-speed shortening with such a small fraction of strongly attached cross-bridges are consistent with conventional cross-bridge models. Therefore, there is no need for multiple force-generating cycles during each biochemical cycle, as suggested by previous studies of isotonic stiffness and fiber ATPase (Higuchi and Goldman, 1991, 1995). Parts of the present study have been reported previously to the Biophysical Society (Stehle et al., 1993; Stehle and Brenner, 1994).

MATERIALS AND METHODS

Fiber preparation and apparatus

Single fibers from rabbit psoas muscle were prepared and chemically skinned with Triton X-100 according to a method described earlier (Yu and Brenner, 1989). The mechanical measurements were performed with an apparatus described by Brenner (1980) and Brenner et al. (1986a). To reduce deterioration of the striation pattern during activation, ~0.5 mm of the fibers at each end were stabilized by a procedure derived from the protocol of Chase and Kushmerick (1988), using a prerigor solution containing an additional 5 vol. % glutaraldehyde as the fixative and 10 vol. % toluidin blue as the optical marker. This solution was applied to the fiber ends by a micropipette that was pulled from a single capillary (4″, 1.2 mm; World Precision Instruments, Sarasota, FL) after the fibers had been transferred to a standard prerigor solution. The higher density of the solution with fixative and dye produced a rapid vertical flow that ensured quick removal of the fixative from the area near the fiber. During activation, the striation pattern was continuously stabilized by a previously described protocol (Brenner, 1983a).

Solutions

All solutions were composed to give a final formal ionic strength (μ) of 170 mM and adjusted to pH_a 7.0 at 5°C. Imidazole and ATP were added as stock solutions adjusted to pH 7 by ~0.6 mol HCl per mol imidazole or 1.7 mol KOH per mol ATP, respectively. Creatine phosphokinase (CPK), hexokinase (HK), and K-glutathione were added immediately before the experiment.

Prerigor solution contained 2.5 mM K_2EGTA, 7.5 mM Na_2EDTA, 135 mM K-propionate, and 10 mM $Cl_{0.6}$-imidazole; rigor solution contained 2.5 mM K_2EGTA, 2.5 mM Na_2EDTA, 150 mM K-propionate, and 10 mM $Cl_{0.6}$-imidazole. For the results shown in Fig. 2 the activating (or relaxing) solution contained 3 mM Ca-K_2EGTA (or 3 mM K_2EGTA), 3 mM $MgCl_2$, 1 mM $Na_2K_{1.7}MgCl_2ATP$, 37.7 mM Na_2CP, 30 mM K-glutathione, 10 mM caffeine, 10 mM $Cl_{0.6}$-imidazole, and 1000 units CPK/ml. To produce solutions containing inorganic phosphate (cf. Fig. 9, *A* and *C*) with the same μ, Na_2CP was replaced by P_i in a molar ratio of 2:3. Activating (or relaxing) solutions with different concentrations of MgATP (cf. Fig. 3) were obtained from stock solutions with 3 mM Ca-K_2EGTA (or 3 mM K_2EGTA), 3 mM $MgCl_2$, 34.4 mM Na_2CP, 10 mM caffeine, and 10 mM $Cl_{0.6}$-imidazole by adding different mixtures of $Na_2K_{1.7}MgCl_2ATP$ and Na_2CP (including 2 mol KCl/mol CP) with a total concentration of 5 mM. One thousand units CPK/ml and 30 mM K-glutathione were added immediately before the experiment.

To ensure the highest possible nucleotide saturation of cross-bridges with MgATPγS, the experiments shown in Figs. 4, *A* and *B*; 5, *A* and *B*; 6, *A–D*; 7; 8; 9, *B* and *D*; and 10 were carried out at −1°C in the presence of high nucleotide concentrations (10 mM; cf. Kraft et al., 1992). The ionic background was switched from CP to propionate to prevent resynthesis of ATP by endogenous CPK when ATPγS was used. ATPγS solutions at high/(or low) Ca^{2+} concentrations: 3 mM Ca-K_2EGTA (or 3 mM K_2EGTA), 3 mM $MgCl_2$, 10 mM $MgCl_2$-Li_4ATPγS, 65 mM K-propionate, 30 mM K-glutathione, 10 mM caffeine, 10 mM $Cl_{0.6}$-imidazole, 0.2 mM Ap_5A, 200 mM glucose, 0.5 units HK/ml. Before use, ATPγS (Boehringer Mannheim, Mannheim, Germany) was purified according to the method of Kraft et al. (1992) by ion-exchange chromatography to remove AMD, ADP, and ATP. For direct comparison, activating or relaxing solutions were used with the same ionic background as the ATPγS-solutions: 3 mM Ca-K_2EGTA (or 3 mM K_2EGTA), 3 mM $MgCl_2$, 10 mM Na_2CP, 10 mM $K_{1.7}$MgATP, 20 mM LiCl, 20 mM Li -propionate, 15 mM K-propionate,

30 mM K-glutathione, 10 mM caffeine, 10 mM $Cl_{0.6}$-imidazole, 0.2 mM Ap_5A, 200 mM glucose, 500 units CPK/ml.

Sarcomere length measurement

Sarcomere length was measured by laser light diffraction with a 4-mW He-Ne laser (Spectra-Physics, Mountain View, CA). To minimize a possible time delay of tension response over the imposed change in sarcomere length, the laser beam was collimated onto the fiber in a region near the force transducer but still within the part of the fiber that was not treated by the fixative. One of the two first-order maxima was imaged on a lateral-effect-type PIN photodiode (SC/10D; United Detector Technology, Santa Monica, CA). Sarcomere length was calculated from the position signal of the photodiode by an analog circuit with a total bandwidth of 70 kHz.

Within a single fiber, the sarcomere pattern consists of several domains, each showing a different tilt of the striation and/or sarcomere lengths. This can be demonstrated by recording the intensity of one first-order maximum as a function of the angle ω between the laser beam and the normal to the fiber axis (Rüdel and Zite-Ferenczy, 1979; Brenner, 1985; Brenner et al., 1986a). However, the sarcomere length measured at a single incidence angle only gives information about the sarcomere length of those domains that satisfy Bragg's law. To obtain a sarcomere length signal representative of the whole fiber cross section (cf. Brenner, 1991, 1998), sarcomere length measurements were performed at various incidence angles ω by tilting the fiber to different angles by steps of ~0.5°. The sarcomere length signals recorded at each of the different incident angles were summed up with the averaging routine of a digital storage oscilloscope (4094/4562/XF-44; Nicolet, Madison, WI).

Stiffness measurement

Fiber stiffness was measured by applying ramp-shaped stretches at velocities of 10^0 to 4×10^4 nm per half-sarcomere (h.s.) per s. Apparent stiffness was defined as the force increment over filament sliding when filament sliding during the ramp-shaped stretches had reached 2 nm (chord stiffness). For isotonic stiffness measurements the length change is regarded as a change in sarcomere length superimposed while the fiber is shortening steadily (Fig. 1). Therefore, the magnitude of the imposed length change was defined as the difference between the actual sarcomere length signal and the sarcomere length obtained by extrapolation of the signal recorded before initiation of the stiffness measurement. To allow direct comparison of isotonic fiber stiffness determined by this technique with stiffness when fibers are not actively shortening (e.g., in the presence of ATPγS), fibers that were not actively contracting were stretched to sufficiently long sarcomere lengths (~2.65 μm) such that passive forces induced filament sliding of similar speeds, as during active contraction (e.g., Fig. 6).

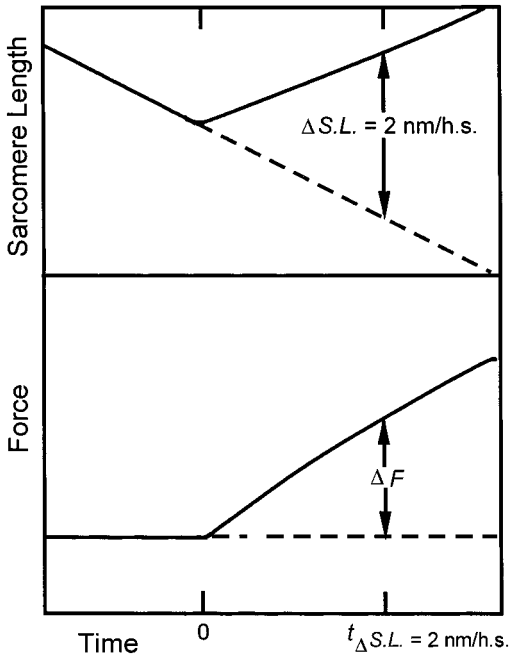

FIGURE 1 Definition of apparent fiber stiffness measured during fiber shortening. First, the sarcomere length signal recorded before initiation of the length change ($t < 0$) was extrapolated to the period during the imposed length change ($t > 0$, indicated by the *dashed line*). Then the time is determined at which the actual sarcomere length had changed by 2 nm per half-sarcomere (h.s.) relative to the extrapolated sarcomere length ($t_{\Delta S.L.}$ = 2 nm/h.s.), and the corresponding change in force (ΔF) is determined. Stiffness is then defined as the ratio $\Delta F/\Delta$S.L. (= 2 nm/h.s.). Note that this definition is equivalent to the chord stiffness determined when filament sliding during the imposed stretch has reached 2.0 nm/h.s. as long as speeds of stretch are much faster than fiber shortening; i.e., for isometric stiffness at all speeds of stretch and for isotonic stiffness at velocities of stretch greater than $10^{3.5}$ nm/h.s./s.

RESULTS

Actin-binding kinetics of cross-bridges during active high-speed shortening

To test whether the actin-binding kinetics of cross-bridges observed during isotonic shortening are different from those seen during isometric contraction, we measured fiber stiffness during isotonic contractions at low load (5 ± 2% of isometric force). Velocity of stretch was varied from 3×10^2 to 3×10^4 (nm/h.s.)/s to obtain stiffness-speed relations for comparison with those observed during isometric contraction and under relaxing conditions (Fig. 2). At a stretch velocity of 1.0×10^4 (nm/h.s.)/s isotonic stiffness is 18.5 ± 1.0% of isometric stiffness. The velocity of active fiber shortening is 0.91 ± 0.05 (μm/h.s.)/s (mean ± SEM; n = 13). These values are in agreement with previous measurements on skinned fibers of the rabbit psoas muscle under similar conditions (μ = 170 mM, T = 5°C; Brenner, 1983b).

If the difference between isometric and isotonic stiffness were simply the result of a decrease in the fraction of strongly bound cross-bridges (Brenner, 1986, 1991), the isotonic stiffness-speed relation would be expected to essentially superimpose on the isometric stiffness-speed relation if properly scaled up. However, as indicated by the solid line in Fig. 2, the isotonic stiffness-speed relation cannot be made to superimpose on the isometric stiffness-speed relation. Instead, the isotonic stiffness-speed relation appears to be shifted by about two orders of magnitude to higher speeds of stretch. Such a shift in the stiffness-speed relation would be expected if cross-bridges attached during high-speed shortening were to detach ~100 times faster from actin than cross-bridges formed during isometric contraction (cf. Schoenberg, 1985; Brenner, 1990). The data of

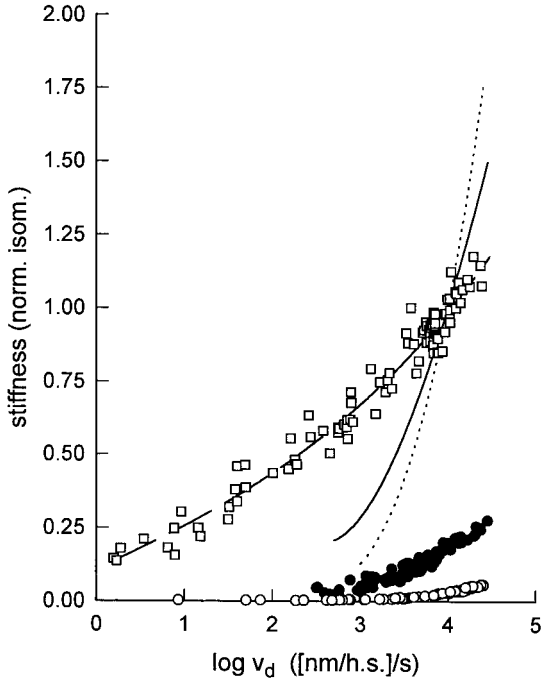

FIGURE 2 Speed dependence of observed fiber stiffness at different contraction conditions. The plot shows the stiffness of 15 fibers measured at 5°C, μ = 170 mM, and at resting sarcomere lengths (2.3–2.4 μm). All data points are normalized to stiffness measured during isometric steady-state contraction at a stretch velocity of 1×10^4 (nm/h.s.)/s. □, Isometric stiffness; ●, isotonic stiffness at 5 ± 2% load relative to isometric force; ○, relaxed stiffness. At a stretch velocity of 1×10^4 (nm/h.s.)/s, stiffness measured during isotonic steady-state shortening is 18.5 ± 1.0% (mean ± SEM; n = 13), and relaxed stiffness is 2.7 ± 0.3% (n = 8) of isometric stiffness. Lines indicate the speed dependence of stiffness when stiffness-speed relations are normalized with respect to their stiffness measured at a stretch velocity of 1×10^4 (nm/h.s.)/s. Scaling factors used: 1 for isometric stiffness-speed relation (– – –); isotonic stiffness-speed relation scaled up 5.4-fold (——); relaxed relation scaled up 37-fold (· · · · ·). Note that both isotonic and relaxed stiffness-speed relations are shifted to higher speeds of stretch relative to the isometric relation; the relaxed relation are shifted the farthest. This is indicated by the crossing over of the three relations.

Fig. 2, however, do not allow us to distinguish whether the relaxed stiffness-speed relation is shifted along the abscissa to faster stretch velocities or scaled down vertically because of less attachment. In any case, these data suggest that actin binding kinetics of cross-bridges attached during high-speed shortening are different from actin-binding kinetics observed during isometric contraction and under relaxing conditions. To elucidate the basis for the observed differences, additional characterization of the stiffness-speed profile was necessary.

Effect of substrate concentration upon actin-binding kinetics of cross-bridges

To develop an understanding for the differences between the stiffness-speed relations obtained during high-speed shortening at low loads versus relaxing conditions, we first checked for possible effects from incomplete nucleotide saturation. In a previous study it was found that nucleotide affinity of myosin heads for the ATP analog MgATPγS became much reduced upon Ca^{2+} activation of the contractile system (Kraft et al., 1992). To rule out effects from gradients in [MgATP] due to hydrolysis within the fiber, especially at low substrate concentrations, we first examined the dependence of isotonic shortening velocity on activity of CPK at various ATP concentrations (plots not shown). Under conditions of lightly loaded (5% of isometric force) shortening and at 0.1 mM MgATP, 1.000 units/ml (definition by Sigma for 30°C and pH 7.4) of CPK from rabbit muscle were needed to obtain a velocity that was independent of the amount of CPK added to the activating solution. In the presence of such high CPK activity, we found (Fig. 3) that stiffness under relaxing conditions is unaffected between 1 and 0.1 mM MgATP, suggesting complete saturation of cross-bridges with MgATP at low Ca^{2+} concentration (pCa $<$ 8). Over the same range of [MgATP], isotonic stiffness-speed relations are shifted up-

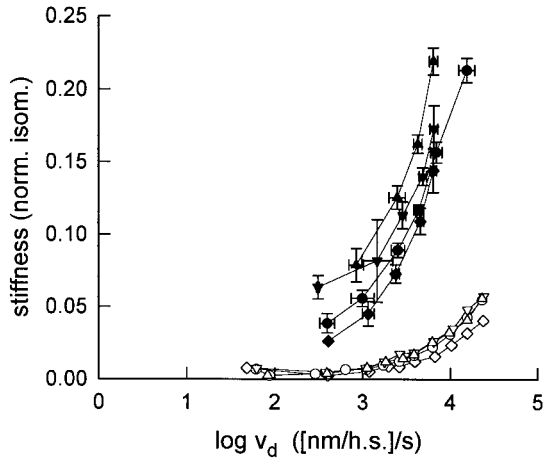

FIGURE 3 Effect of MgATP concentration on isotonic and relaxed stiffness-speed relations, under the same conditions (T, μ, and sarcomere length) as in Fig. 2. Stiffness is normalized to stiffness measured during isometric contraction in the presence of 1 mM MgATP at a stretch velocity of 1×10^4 (nm/h.s.)/s. Data were pooled from 16 fibers. Points plotted are means of 2–21 single measurements and are obtained by grouping data from single stiffness measurements at similar speeds of stretch. Filled symbols represent isotonic stiffness data measured at 5 ± 2% load (relative to isometric force); open symbols represent relaxed fiber stiffness. Different symbols represent different concentrations of MgATP: 0.1 mM (▲, △); 0.25 mM (▼, ▽); 1 mM (●, ○), and 5 mM (◆, ◇). Error bars represent SEM for stiffness and SD for speed of stretch. In case of relaxed stiffness, error bars are within the size of the symbols. For concentrations of substrate below 1 mM, isotonic relations appear to be shifted upward by an extra amount of stiffness. This indicates an "extra stiffness" resulting from slowly detaching cross-bridges, suggesting that substrate binding starts to limit cross-bridge detachment below 1 mM MgATP. At MgATP concentrations above 1 mM no further change in the difference between isotonic and relaxed stiffness-speed relations is observed. This suggests that the difference between the stiffness-speed relations for high-speed shortening and relaxed conditions does not result from limited saturation with substrate.

ward when the substrate concentration is reduced, as expected for incomplete nucleotide saturation. Raising [MgATP] from 1 to 5 mM results in a slight decrease in fiber stiffness for both active isotonic and relaxed conditions. This decrease is ~1% of the stiffness observed under active isometric contraction and is presumably due to either an unspecific MgATP effect or an ionic strength effect when CP is exchanged for MgATP. However, most importantly, increasing the MgATP concentration from 1 to 5 mM does not bring the isotonic and relaxed stiffness-speed relations significantly closer. Furthermore, increasing [MgATP] within this range does not further increase the velocity of isotonic shortening under our conditions; the shortening velocity at 5 mM MgATP was 0.97 ± 0.02 (mean ± SEM; $n = 6$) of that measured at 1 mM MgATP. Together, these findings indicate that limited substrate concentration does not account for the differences found between relaxed and isotonic stiffness-speed relations at low loads (Fig. 2).

Effect of load on stiffness-speed relations and estimation of actin-binding kinetics for unloaded shortening

So far we have determined isotonic stiffness-speed relations only in the presence of small external loads. Presumably, filament sliding against these loads must be driven by force-generating cross-bridges present in addition to those driving filament sliding under truly unloaded conditions. To characterize detachment kinetics of cross-bridges present during shortening at v_{max}, it is necessary to derive stiffness-speed relations for truly unloaded conditions. At truly zero external load, however, fiber stiffness cannot be measured directly, because fibers tend to go slack at very low loads, so that the laser diffraction signal for recording of the sarcomere length is lost. As an alternative, we derived the isotonic stiffness-speed relation for unloaded conditions from a series of stiffness measurements recorded under different loads. To do so, we first plotted apparent fiber stiffness versus load (Fig. 4 *A*), using stiffness data obtained for five different velocities of stretch ($10^{2.5}$, $10^{3.0}$, $10^{3.5}$, $10^{4.0}$, and $10^{4.5}$ (nm/h.s.)/s). Each of the five resulting plots of fiber stiffness versus load was extrapolated for zero load, using a linear regression (Fig. 4 *A*). The extrapolated stiffness values are plotted versus speed of stretch (Fig. 4 *B*, *small filled circles*) and compared with the stiffness-speed relations recorded during isotonic shortening at the different loads, during isometric contraction and under relaxing conditions. With decreasing loads the observed fiber stiffness becomes smaller (Fig. 4 *B*), and compared with stiffness-speed relations recorded at higher loads, those at reduced loads appear to be shifted to higher speeds of stretch rather than scaled

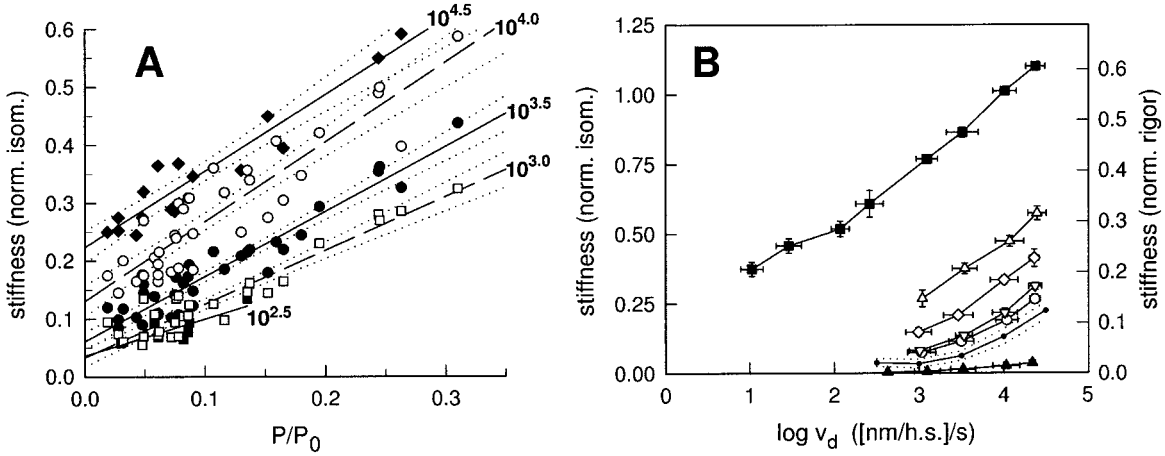

FIGURE 4 Effect of load on isotonic stiffness and its dependence upon speed of stretch. Measurements were performed at −1°C, $\mu = 170$ mM, and S.L. of 2.55–2.65 μm to allow for further comparison with stiffness-speed relations recorded with MgATPγS at high [Ca^{2+}] (cf. Fig. 7). All stiffness values are normalized to isometric stiffness measured at the same conditions at a stretch velocity of 1×10^4 (nm/h.s.)/s. (*A*) Estimate of stiffness for unloaded isotonic shortening from plots of apparent fiber stiffness versus relative load. To plot stiffness versus load at the distinct speeds of stretch, a series of stiffness-speed relations, each measured on an individual fiber (17 in total) in the presence of the same load, was plotted (not shown), and isotonic stiffness was evaluated by interpolation for the preselected speeds of stretch (in (nm/h.s.)/s): $10^{2.5}$ (■), $10^{3.0}$ (□), $10^{3.5}$ (●), $10^{4.0}$ (○), and $10^{4.5}$ (♦). Solid and dashed lines are linear regressions fitted to the data to determine the expected stiffness for unloaded shortening. Dotted lines indicate the 95% confidence limits of each regression. (*B*) Stiffness-speed relations measured during isometric contraction (■), isotonic contraction at four different loads (△, ◇, ▽, ○), and relaxed conditions (▲), plotted together with the relation derived for fully unloaded shortening, i.e., at v_{max} (—•—). Data are from the same fibers as in Fig. 4 *A*. Relative loads (P/P_0): 20–25% (△), 10–15% (◇), 5–7.5% (▽), and 2.5–5% (○). Each point represents the mean of 3–35 (isometric), 2–10 (relaxed), or 3–16 (isotonic) stiffness measurements. Error bars: ± SEM (stiffness) or ± SD (velocity of stretch). The stiffness-speed relation for active unloaded shortening (—•—) was derived from the values of the regression lines shown in Fig. 4 *A*, extrapolated for zero load. Dashed lines connect the 95% confidence limits of the regression lines at zero load shown in Fig. 4 *A*. The second scale for the ordinate shows normalization to rigor stiffness. This normalization is derived from the observation that isometric stiffness at the stretch velocity used for normalization (10^4 (nm/h.s.)/s) is 55 ± 10% (mean ± SEM; $n = 4$) of rigor stiffness at the present experimental conditions ($T = -1$°C, $\mu = 170$ mM, S.L. = 2.6 μm).

down vertically. This suggests that overall the cross-bridge population present at low loads apparently detaches faster. This may result from either faster reversible detachment of strongly bound cross-bridges or from a smaller contribution of strongly binding cross-bridges to fiber stiffness compared to the contribution of weakly binding cross-bridges at the lower loads.

To distinguish between these two alternatives we attempted to determine whether force-generating cross-bridges present during isotonic shortening at low loads have detachment kinetics different from those present during isometric contraction. The analysis is based on the assumption that the "extra stiffness" observed during shortening under loaded versus unloaded conditions results from strongly bound cross-bridges necessary to drive filament sliding against the "extra" external load. The stiffness-speed relation of this "extra stiffness" is assumed to provide information about the actin-binding kinetics of force-generating cross-bridges present during isotonic conditions. For the four different loads (cf. Fig. 4) the "extra stiffness" beyond the stiffness extrapolated for completely unloaded conditions was determined and plotted versus speed of stretch. The resulting stiffness-speed relations are shown in Fig. 5 *A*.

In Fig. 5 *B*, these stiffness-speed relations are compared with the stiffness-speed relation seen during isometric contraction and the stiffness-speed relation derived for unloaded conditions. All stiffness-speed relations were normalized for the stiffness observed at a speed of stretch of 10^4 (nm/h.s.)/s. Fig. 5 *B* demonstrates that the "extra fiber stiffness" observed during loaded shortening shows a dependence on velocity of stretch similar to that of the fiber stiffness recorded during isometric contraction but appears distinctly different from the stiffness-speed relation derived for unloaded conditions.

Thus isotonic stiffness-speed relations recorded under loaded shortening may be visualized as resulting from two cross-bridge populations, one population with a speed-dependence of stiffness similar to that observed under isometric conditions, the other characterized by a speed dependence of stiffness that is shifted by about two orders of magnitude to faster stretch velocities, but which is still different from that of relaxed fibers (cf. Fig. 4 *B*, *small filled circles* versus *filled triangles*).

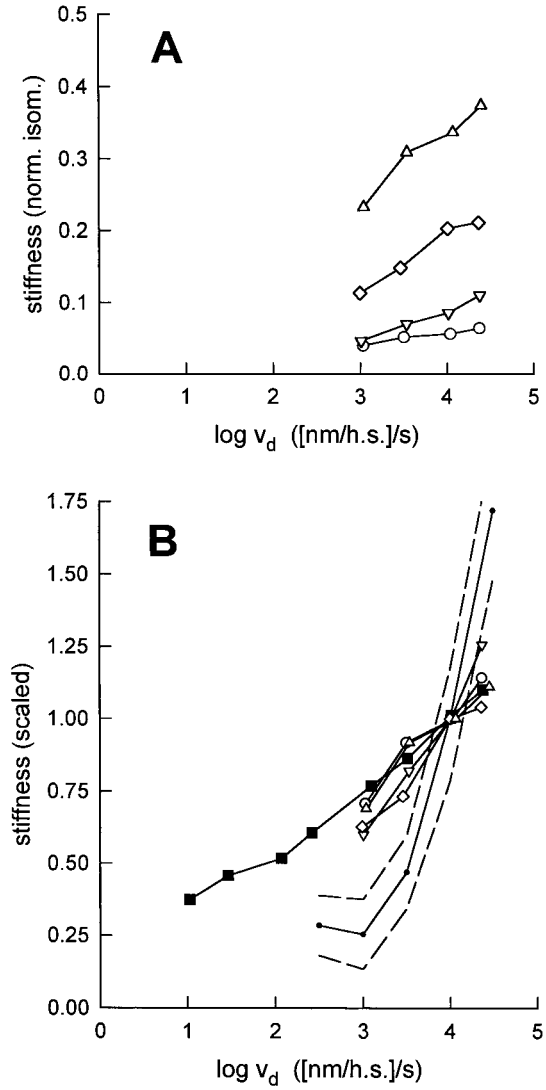

FIGURE 5 Analysis of the speed dependence of "extra stiffness" arising from the presence of load during active isotonic shortening. (*A*) Speed dependence of "extra stiffness" derived from Fig. 4 *B* by subtracting, for each speed of stretch, the extrapolated unloaded stiffness from stiffness observed during isotonic shortening at loads of P/P_0 = 20–25% (△), 10–15% (◇), 5–7.5% (▽), and 2.5–5% (○). (*B*) The plots of Fig. 5 *A* (*open symbols*) shown together with the relations for isometric contraction (■) and the extrapolated values for unloaded shortening (—•—). Data of all conditions are normalized with respect to their values at a speed of stretch of 1×10^4 (nm/h.s.)/s. Dashed lines represent 95% confidence limits of the extrapolated relation for unloaded shortening. Speed dependences of "extra stiffness" observed during shortening at the four different loads are close to the isometric stiffness-speed relation. The cross-overs between the stiffness-speed relation derived for unloaded conditions and the isometric stiffness-speed relation plus the speed dependences of "extra stiffness" indicate that the stiffness-speed relation for unloaded conditions is shifted to higher stretch velocities (at least two orders of magnitude).

Stiffness-speed relations for unloaded shortening versus stiffness-speed relations in the presence of MgATPγS

At all speeds of stretch the stiffness extrapolated for unloaded shortening is much higher than relaxed fiber stiffness (see Fig. 4 *B*). This indicates that the cross-bridge population present under conditions of unloaded shortening has properties that differ from those of both the population present under isometric conditions and the cross-bridges responsible for stiffness under relaxing conditions. However, using the slowly hydrolyzed ATP analog ATPγS (Bagshaw et al., 1972, 1974; Goody and Hofmann, 1980), it was recently found that actin-binding kinetics of weakly

binding cross-bridges are slowed down considerably upon Ca^{2+} activation, resulting in a shift of the stiffness-speed relation toward lower speeds of stretch (Kraft et al., 1992). To test whether the cross-bridges present under unloaded shortening conditions may have properties similar to those of cross-bridges in weakly binding states but under full Ca^{2+} activation, we compared the stiffness-speed relation derived for unloaded shortening conditions with the stiffness-speed relation in the presence of MgATPγS at high [Ca^{2+}], using MgATPγS as a nucleotide analog for generating weakly binding states, even under activating Ca^{2+} concentrations (Kraft et al., 1992). To still provide sufficient nucleotide saturation despite the much reduced nucleotide affinity in the presence of Ca^{2+}, we had to use 10 mM MgATPγS and reduce temperature as much as possible (to -1°C; Kraft et al., 1992). To account for the possible effects of filament sliding per se on the observed stiffness-speed relations, we developed a protocol that allowed us to measure fiber stiffness in relaxed fibers (ATP, low [Ca^{2+}]) or in the presence of MgATPγS (either at low or high [Ca^{2+}]) during a period of passive shortening by which the a velocity of filament sliding is generated that is the same as that observed during active shortening at low loads (Fig. 6).

Using this protocol, no effect upon stiffness-speed relations is found when MgATP is replaced by MgATPγS in the absence of Ca^{2+} (Fig. 7), in agreement with previous work without filament sliding (Kraft et al., 1992). This suggests that cross-bridges with either MgATPγS or MgATP/MgADP·P_i bound to their active site have similar actin-binding kinetics under relaxing conditions, both with and without filament sliding. Increasing calcium in the presence of MgATPγS from pCa < 8 to levels necessary for full Ca^{2+} activation (pCa $\approx$ 4.5) results in an increase in fiber stiffness close to the values derived for active shortening under zero load (Fig. 7). The very close agreement of the stiffness-speed relation derived for unloaded isotonic shortening with that observed in the presence of MgATPγS at maximum Ca^{2+} activation is consistent with a concept in which fiber stiffness during active unloaded shortening predominantly arises from weakly bound cross-bridges with actin binding kinetics similar to those seen in the presence of MgATPγS at saturating [Ca^{2+}] (pCa $\approx$ 4.5). The very close observed agreement in the stiffness-speed relations only leaves room for a very small population of strongly attached cross-bridges contributing to fiber stiffness during unloaded shortening. From comparison with the stiffness-speed relation recorded for isometric steady-state contraction (Fig. 4 *B*) it appears that $<5\%$ of the strongly attached cross-bridges present during isometric contraction can contribute to the stiffness-speed relation derived for unloaded shortening. Scatter of the data, however, makes a more precise estimate impossible.

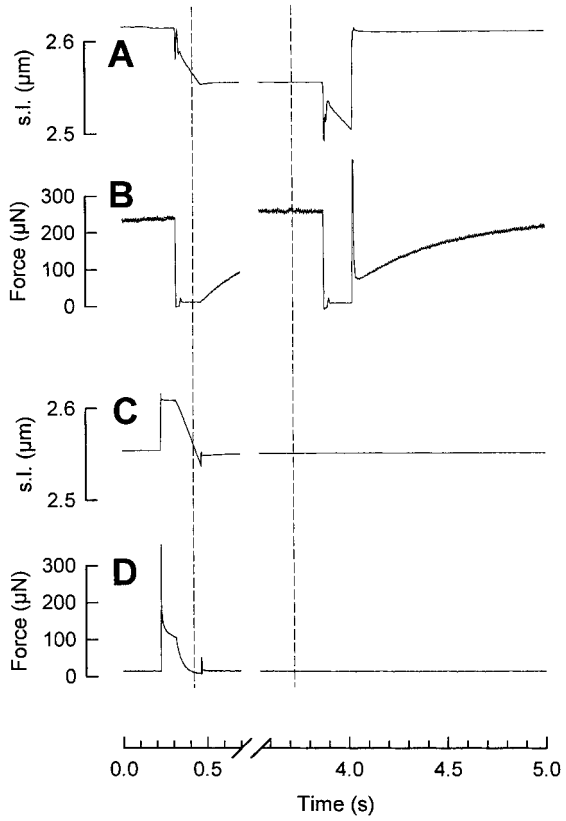

FIGURE 6 Experimental protocol to perform stiffness measurements during active isotonic shortening in the presence of MgATP and during passive shortening under relaxing conditions or in the presence of MgATPγS ($\pm$ Ca^{2+}) at comparable velocities of filament sliding and similar sarcomere length. $T = -1$°C, $\mu = 170$ mM. (*A*) Sarcomere length signal of an activated fiber (pCa $\approx$ 4.5) in the presence of 10 mM MgATP. Isotonic stiffness was measured 100 ms after the initiation of shortening (indicated by the *dashed line* at 0.4 s). Isometric stiffness was measured at a similar sarcomere length at the time indicated by the dashed line at 3.7 s. To restretch fibers to their initial length without damage, a second period of isotonic shortening was applied. Immediately after the initiation of isotonic release the fiber went slack for 15 ms (force level = zero). During this period the sarcomere length signal shows artifacts due to the movement of the fiber out of the laser beam. (*B*) Force signal corresponding to *A*. Zero tension was determinated from the signal during the first 15 ms after initiation of shortening when fibers go slack. (*C*) Sarcomere length signal of the same fiber in the presence of 10 mM MgATPγS at high [Ca^{2+}] (pCa 4.5). Passive shortening was initiated after a transient stretch to sarcomere lengths of 2.6–2.65 μm. (*D*) Force signal corresponding to *C*. Note that fibers develop no active isometric force in the presence of MgATPγS at both high and low [Ca^{2+}] (data for low [Ca^{2+}] are not shown).

Further evidence that fiber stiffness during unloaded shortening predominantly reflects weak cross-bridge attachment

1. We had to rule out that the stiffness-speed relation for unloaded shortening appears to be shifted to higher stretch velocities simply because non-cross-bridge factors like viscoelastic properties become more predominant when the number of strongly attached cross-bridges is much reduced.

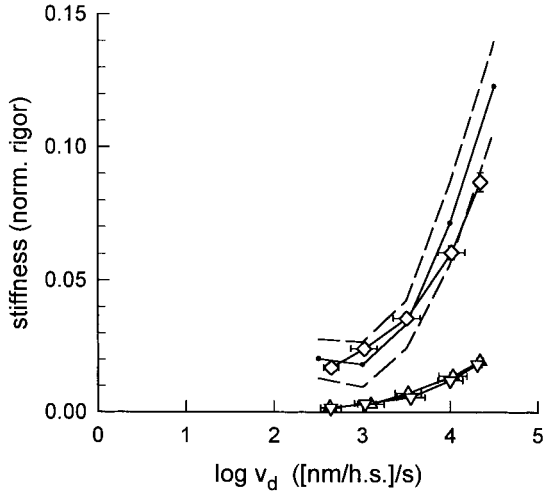

FIGURE 7 Comparison of the stiffness-speed relation extrapolated for unloaded active shortening with those measured during passive shortening at similar velocities, and the effect of nucleotide and Ca^{2+}. All stiffness values are normalized to rigor stiffness. $T = -1°C$, $\mu = 170$ mM, S.L. = 2.5–2.6 μm. △, ▽, Stiffness during passive shortening at low [Ca^{2+}] (pCa < 8), in the presence of 10 mM MgATP (△) or 10 mM MgATPγS (▽); ◇, stiffness during passive shortening at pCa ≈ 4.5 in the presence of 10 mM MgATPγS; —•—, stiffness derived for active unloaded shortening at pCa ≈ 4.5 in the presence of 10 mM MgATP (data from Fig. 4 *B*). The dashed lines represent 95% confidence limits (cf. Fig. 4 *B*). Each point represents the mean ± SEM of 5–23 stiffness measurements.

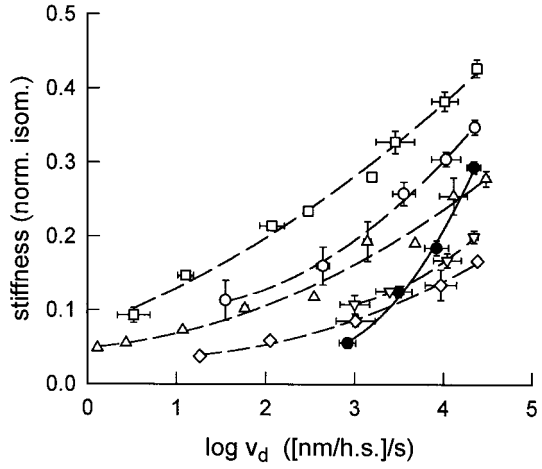

FIGURE 8 Comparison of isotonic stiffness-speed relation (measured at full Ca^{2+} activation) with relations for isometric stiffness of similar low magnitude achieved by only partially activating with Ca^{2+}. All stiffness data are normalized to isometric stiffness measured at full Ca^{2+} activation and at a speed of stretch of 10^4 (nm/h.s.)/s. Experiments were performed at $-1°C$, $\mu = 170$ mM, and at sarcomere lengths of 2.6 μm. Open symbols represent isometric stiffness measured at partial Ca^{2+} activation resulting in isometric force levels (% of full Ca^{2+} activation) of 9–12% (– –◇– –), 13–16% (– –▽– –), 25–26% (– –△– –), 28% (– –○– –), and 40–42% (– –□– –). Isotonic stiffness (—●—) was measured during shortening at 5 ± 2% load relative to isometric force. Each of the five isometric relations was obtained from one fiber. The isotonic relation contains data collected from all five fibers. Symbols represent mean of 1–8 (isometric) or 5–16 (isotonic) stiffness measurements; error bars represent ± SEM (stiffness) and SD (speed of stretch). Note that although amplitude of isometric stiffness is close to isotonic stiffness, all isometric relations show very different dependences on speed of stretch compared to the isotonic relation recorded under low load.

We therefore examined the stiffness-speed relation of fibers that were only partially activated. By lowering the Ca^{2+} concentration, we reduced isometric fiber stiffness to values similar to those observed during active shortening at low loads but at full Ca^{2+} activation. Comparison of the stiffness-speed relations at partial Ca^{2+} activation with that observed under high-speed shortening at full Ca^{2+} activation demonstrates that even for a similar magnitude of fiber stiffness the isotonic stiffness-speed relation is still shifted to higher stretch velocities compared to isometric stiffness (Fig. 8). The speed dependence of isometric fiber stiffness at these low stiffness levels is not significantly different from that observed at maximum Ca^{2+} activation (normalized stiffness-speed relations essentially superimpose; data not shown). This makes it unlikely that the shift of the stiffness-speed relation for unloaded shortening results from non-cross-bridge phenomena (like viscoelastic components) becoming more predominant if only few cross-bridges are strongly attached.

2. If stiffness at v_{max} is indeed dominated by weakly bound cross-bridges, then any decrease or increase in the fraction of strongly bound cross-bridges under isometric conditions may have little or no effect on stiffness during unloaded shortening. We therefore used different interventions to reduce the fraction of force-generating cross-bridges during isometric contraction and attempted to determine whether these interventions also affect fiber stiffness during active shortening near zero load.

Adding 7.5 mM inorganic phosphate (P_i) to the activating solution (Fig. 9 *A*) and decreasing temperature (*T*) from 5°C to −1°C (Fig. 9 *B*) both decreased isometric stiffness at all speeds of stretch by ~30%. This reduction in isometric stiffness indicates a significant reduction of strongly bound cross-bridges by both interventions. If stiffness at high-speed shortening would represent strongly bound cross-bridges but with faster detachment kinetics than during isometric contraction, stiffness during isotonic shortening under low loads (2.5–5% at isometric force) may also be affected by these two interventions. If, however, the contribution of strongly bound cross-bridges to fiber stiffness observed for shortening under near-zero load is very small, neither intervention would much affect the unloaded stiffness-speed relation. Fig. 9, *A* and *B*, show that stiffness-speed relations observed during low-loaded shortening are not significantly affected by either increasing [P_i] or decreasing *T*.

Fig. 9, *C* and *D*, demonstrate the effects of [P_i] and *T* extrapolated for zero load. Fiber stiffness was measured at different loads by fast stretch velocities (10^4 (nm/h.s.)/s). The stiffness extrapolated for zero load is much less af-

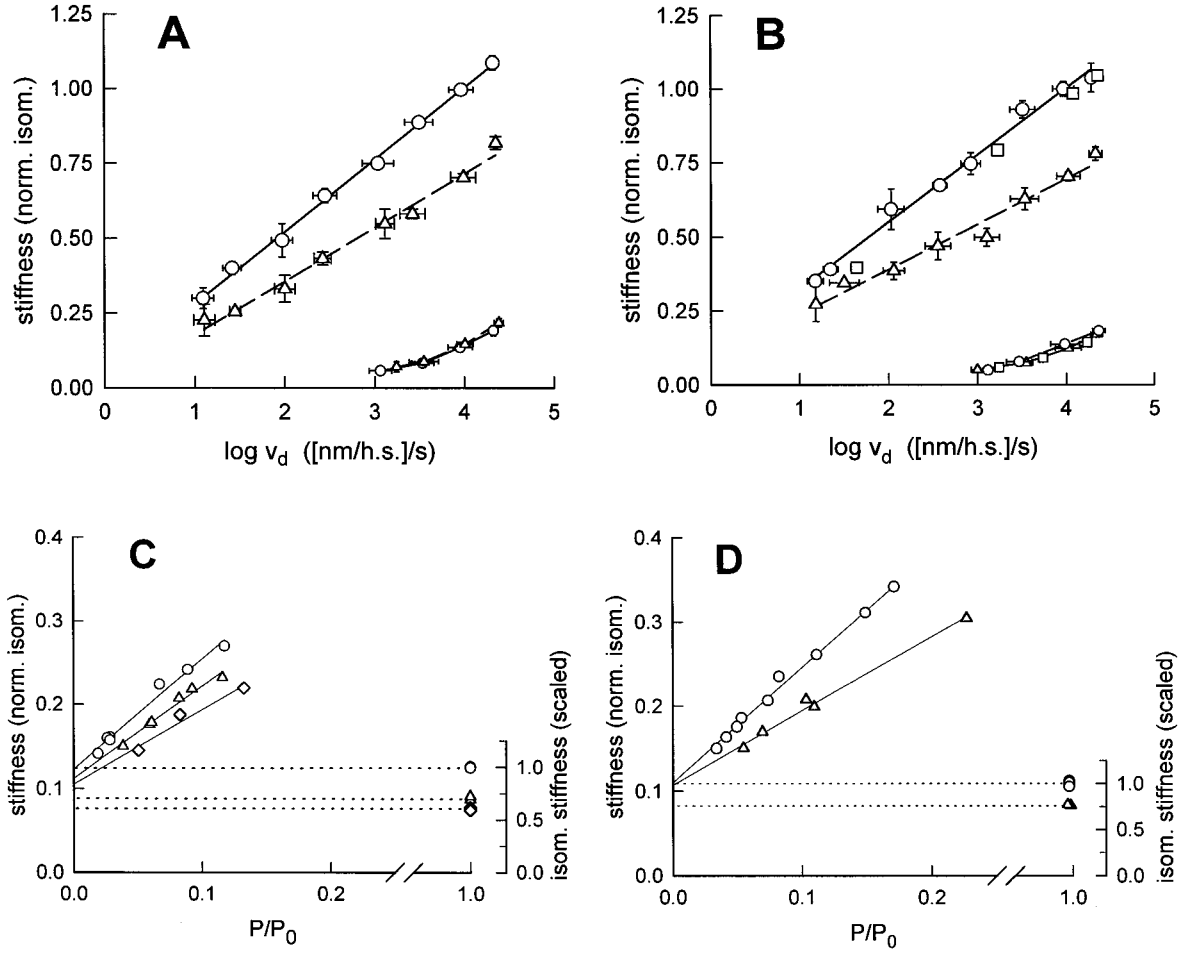

FIGURE 9 Effect of inorganic phosphate (P_i) and temperature (T) on isometric stiffness and on isotonic stiffness measured at low loads. (*A*) Effect of P_i on stiffness-speed relations (T = 5°C, μ = 170 mM). No added P_i (—○—), 7.5 mM P_i (– –△– –). Larger symbols represent isometric stiffness, small symbols isotonic stiffness. Isotonic stiffness was measured under loads of 5 ± 2% of isometric force observed without and with 7.5 mM P_i, respectively. Data were pooled from nine fibers; symbols represent means of 2–16 stiffness measurements. Error bars are ± SEM for stiffness and ± SD for speed of stretch. All stiffness data are normalized to isometric stiffness measured at 10^4 (nm/h.s.)/s without additional P_i. The addition of 7.5 mM P_i reduced isometric force to 57 ± 2% of its original value and decreased isometric stiffness by 30% at all speeds of stretch. Isotonic stiffness is not significantly affected by P_i. (*B*) Effect of T on stiffness-speed relations (no added P_i, μ = 170 mM). T was 10°C (□), 5°C (—○—), or −1°C (– –△– –). Larger symbols represent isometric stiffness, small symbols isotonic stiffness measured during shortening. For each temperature, load during shortening was adjusted to 6 ± 1% of the observed isometric force. Data are pooled from seven fibers; symbols represent mean ± SEM (n = 1–15). All stiffness data are normalized to isometric stiffness measured at 5°C at 10^4 (nm/h.s.)/s. Only isometric stiffness was found to be affected significantly, however, only when the temperature was changed between −1°C and 5°C. Despite the fact that decreasing T from 5°C to −1°C reduced velocity of isotonic shortening by a factor of 3, isotonic stiffness measured at 6 ± 1% load changed less than 15% at all speeds of stretch. (*C*) Effect of P_i on unloaded stiffness. The plot shows representative data for one fiber (of a total of four fibers investigated). Experimental conditions and normalization of stiffness are as in *A*. Stiffness was measured at a stretch velocity of 1×10^4 (nm/h.s.)/s. Concentration of P_i added: 0 mM (○), 7.5 mM (△), and 20 mM (◇). Solid lines were obtained by linear regression of isotonic stiffness data to estimate the stiffness at zero load. For comparison of P_i effects on unloaded isotonic stiffness with that on isometric stiffness (*horizontal dotted lines*), stiffness data were adjusted so that in the absence of P_i isometric stiffness matches the extrapolated stiffness for zero load. Dotted lines illustrate the stiffness levels expected if unloaded isotonic stiffness parallels the effects on isometric stiffness. Unloaded stiffness appears to be affected less than half as much as isometric stiffness. (*D*) Effect of decreasing T from 5°C (○) to −1°C (△) on unloaded stiffness. Experimental conditions and normalization according to *B*. The speed of stretch used for stiffness measurement, the scaling, and the meaning of lines are as described in *C*. As in two other experiments (data not shown), unloaded stiffness is not significantly reduced by temperature, while isometric stiffness is always decreased by ~30%.

fected by [P_i] and T than isometric stiffness. This again is consistent with our working hypothesis that during active unloaded shortening strongly bound cross-bridges contribute much less to fiber stiffness than weakly bound cross-bridges.

DISCUSSION

The most relevant findings of this study are 1) that the speed dependence of observed fiber stiffness shifts by about two orders of magnitude toward higher speeds of stretch with

the change from isometric steady-state contraction to high-speed shortening near v_{max}. 2) The stiffness-speed relation derived for unloaded shortening at v_{max} is different from that observed under relaxing conditions or in the presence of MgATPγS at low Ca^{2+} concentrations. It is, however, almost identical to the stiffness-speed relation observed in the presence of MgATPγS at saturating Ca^{2+} concentrations. 3) Our further analysis suggests that during unloaded shortening almost all cross-bridges may occupy weakly binding-type cross-bridge states, as seen in the presence of saturating [MgATPγS] and at high [Ca^{2+}]. On this basis, most of the fiber stiffness observed during unloaded shortening appears to be due to weak cross-bridge attachment to the activated actin filaments.

Interpretation of the stiffness-speed relation observed during high-speed shortening

The observation that the stiffness-speed relation derived for unloaded conditions is very close to that recorded in the presence of MgATPγS at saturating Ca^{2+} concentrations can be accounted for if the stiffness-speed relation for high-speed shortening is assumed to result from two cross-bridge populations that do not interchange on the time scale of the stiffness measurements; the majority represent cross-bridges in weakly binding states with actin binding kinetics similar to those seen for cross-bridges saturated with MgATPγS at high Ca^{2+} concentrations and a rather small population of strongly attached cross-bridges, possibly with actin binding kinetics like those seen under isometric steady-state conditions. This view is supported by the observation that the differences in stiffness-speed relations recorded during shortening under different external loads can be accounted for by a population of strongly attached cross-bridges that increases with the applied load and is characterized by a stiffness-speed relation similar to that seen under isometric conditions (Fig. 5 *B*). On the basis of such a mixed population, comparison of the stiffness-speed relation derived for unloaded conditions with that for cross-bridges in the presence of MgATPγS at high Ca^{2+} concentration indicates that during unloaded shortening there is room for only a small fraction of strongly attached cross-bridges with a stiffness-speed relation like that seen for isometric conditions. Our estimate of Fig. 7 would only allow for $<5\%$ of the population of strongly attached cross-bridges present during isometric contraction. Thus, in this model, most of the stiffness observed during high-speed shortening results from weak cross-bridge attachment, like the attachment seen in the presence of MgATPγS at saturating Ca^{2+} concentrations, while the contribution of strongly attached cross-bridges becomes very small when the external load approaches zero.

Previously, such a significant contribution of weakly attached cross-bridges to the isotonic stiffness was not considered (Brenner, 1983b; Ford et al., 1985; Haugen, 1986; Griffiths et al., 1993). This due to two things: first, stiffness-speed relations for high-speed shortening had not been determined in detail. Second, the previously observed relaxed fiber stiffness is much lower than the isotonic stiffness, such that it was assumed that weak interactions do not contribute significantly. However, it had not been recognized that Ca^{2+} activation, although without much effect on actin affinity, apparently slows down the actin-binding kinetics (dissociation and reassociation) of weakly binding cross-bridges, as seen when raising [Ca^{2+}] in the presence of saturating concentrations of MgATPγS (Kraft et al., 1992). As shown in the present study, the difference in apparent fiber stiffness observed between relaxed fibers and during unloaded shortening may mainly result from the effect of Ca^{2+} activation on actin-binding kinetics of weakly binding cross-bridges.

Based on our previously proposed interpretation of the dependence of observed fiber stiffness on the speed of the applied stretch (stiffness-speed relations; Schoenberg et al., 1984; Schoenberg, 1985, 1988; Brenner et al., 1986a; Brenner, 1990), the stiffness-speed relation observed during high-speed shortening indicates quite fast detachment rate constants of cross-bridges during unloaded shortening conditions, i.e., on the order of $\geq 10^4$ s^{-1}. A more precise estimate, however, is not possible because of the rather limited range of the stiffness-speed relation that can be measured up to now.

Alternative interpretations

As one possible alternative to our above interpretation we have to consider the possibility that the stiffness-speed relation during high-speed shortening results from the detachment of strongly attached cross-bridges being faster during high-speed shortening compared to isometric contraction. This could be due to either rapid completion of the ATPase cycle by fast release of ADP and binding of a new ATP molecule, or forced detachment with reattachment to subsequent sites on actin when strongly attached cross-bridges become negatively strained (e.g., Cooke et al., 1994; Piazzesi and Lombardi, 1995). These alternatives, however, appear to be unlikely because the detachment kinetics upon ADP release or forced detachment are about two orders of magnitude too slow to account for the stiffness-speed relation derived for unloaded conditions. For example, detachment by completion of the cross-bridge cycle in rabbit fibers during unloaded isotonic shortening conditions was found to take place with an apparent rate constant of $\sim$70–150 s^{-1} for the conditions used in this study (Brenner, 1988a, 1993; Brenner and Stehle, 1994). Similarly, the rate constants for forced detachment of force-generating cross-bridges and reattachment to a subsequent binding site on actin were proposed to occur at $\sim$100 s^{-1} (Cooke et al., 1994; Piazzesi and Lombardi, 1995).

Fraction of cross-bridges occupying strongly binding states during unloaded shortening

If we interpret the stiffness-speed relation derived for unloaded isotonic conditions in terms of two cross-bridge populations, i.e., a large fraction of cross-bridges in weakly binding states with actin binding kinetics identical to those observed in the presence of saturating concentrations of MgATPγS at high [Ca^{2+}] and a small fraction with actin binding kinetics as represented by the isometric stiffness-speed relation, the question arises, how large a fraction of strongly binding cross-bridges has to be considered for unloaded shortening compared to isometric steady-state conditions? Comparison of the stiffness-speed relation obtained for unloaded conditions with the stiffness-speed relation observed for MgATPγS at high Ca^{2+} concentrations reveals that the two stiffness-speed relations are almost within experimental error, i.e., that there is little room for a population of strongly attached cross-bridges with a stiffness-speed relation seen under isometric conditions. The data would be consistent with a component of strongly attached cross-bridges on the order of up to some 1–5% of the population present under isometric conditions. This is almost an order of magnitude lower than the value derived in previous studies (cf. Burton, 1992, for a review), the reason for this being the assumption in the previous studies that all of the fiber stiffness originates from cross-bridges in strongly binding states.

The fraction of all cross-bridges that may be strongly attached during unloaded shortening will depend on the fraction of strongly attached cross-bridges present during isometric steady-state contraction. From measurements of fiber stiffness, a large fraction was derived to occupy strongly binding states (Goldman and Simmons, 1977). Filament compliance (Wakabayashi et al., 1994; Huxley et al., 1994; Kojima et al., 1994; Higuchi et al., 1995; Linari et al., 1998) and possible differences in cross-bridge stiffness among various cross-bridge states (e.g., rigor cross-bridge, active force-generating cross-bridge), however, make this estimate somewhat ambiguous. Alternatively, from electron paramagnetic resonance and fluorescence polarization studies it was proposed that the fraction of strongly attached cross-bridges during isometric conditions is rather small (some 10–30%; Cooke et al., 1982; Ostap et al., 1995; Sabido-David et al., 1998).

From stiffness measurements (rigor stiffness versus active isometric stiffness) it is not clear at present what fraction of cross-bridges is strongly attached during isometric steady-state contraction. Thus, on the basis of stiffness measurements, we cannot give an estimate of the fraction of cross-bridges strongly attached during unloaded shortening.

An alternative estimate had been based on the characterization of cross-bridge tunover kinetics, i.e., the apparent rate constants that determine cycling between weak and strong binding states (e.g., f_{app}, g_{app}, etc.), by recording of fiber ATPase and force or stiffness transients during isovelocity contraction (Brenner, 1988a; Brenner and Stehle, 1994). This approach is independent of stiffness measurements and suggests that during high-speed shortening occupancy of strongly binding states is only some 1–5% of that observed during isometric steady-state contraction, consistent with our interpretation of stiffness data presented here. In addition, this analysis again suggests a rather significant fraction of strongly attached cross-bridges during isometric steady-state conditions (some 60–75%; cf. Brenner, 1986). Thus the fraction of cross-bridges in strongly binding states during high-speed shortening estimated by this approach is on the order of 1–3% of the total number of cross-bridges versus 60–75% during isometric steady-state contraction and thus is consistent with our interpretation of stiffness data presented here. With only a small fraction of cross-bridges in strongly binding states during isometric steady-state contraction, it would be difficult, however, to account for the large changes in the stiffness-speed relation when changing to high-speed shortening; i.e., the observed large effects also point to a larger fraction of cross-bridges in strongly binding states during isometric contraction. However, the question of whether all cross-bridges in strongly binding states are also contributing to isometric force (i.e., occupying states in which a significant contribution to isometric force is made and in which cross-bridges might respond to sudden length changes) remains to be examined and may help to resolve the present dispute about high and low fraction of force-generating cross-bridges under isometric conditions. Nevertheless, although this isometric steady-state distribution is still unclear, the relevant conclusion is that stiffness measurements are consistent with the occupancy of strongly binding cross-bridge states during high-speed shortening being less than 5% of that during isometric contraction. Thus, even for a large fraction of strongly attached cross-bridges during isometric contraction, there is no problem with conventional cross-bridge models concerning interaction distances (see below).

Similarly, from an analysis of kinetic parameters of activated freely shortening myofibrils, Ma and Taylor (1994) concluded that only a fraction of cross-bridges as small as a few percent should occupy strongly binding states during unloaded shortening. The apparent discrepancy with stiffness data had been accounted for by Ma and Taylor (1994) and by our preliminary report on the model presented here (Stehle et al., 1993).

Implications for the interaction distance

As already pointed out, the interaction distance, i.e., the distance of filament sliding while a cross-bridge occupies strongly binding force-generating states, has previously been calculated from fiber ATPase and fiber stiffness recorded during high-speed shortening (for a review cf. Burton, 1992). In these previous estimates it was assumed that

all of the fiber stiffness observed during high-speed shortening originates from strong cross-bridge interactions. With a large fraction of cross-bridges in strongly binding states, the stiffness data were interpreted to suggest that some 20–40% of all cross-bridges occupy strongly binding states during unloaded shortening. Correlation with ATP hydrolysis resulted in interaction distances of >40 nm, i.e., much larger than the size of the cross-bridge, thus leading to proposals of reversible actin interactions or multiple power strokes within a single ATPase cycle (cf. Burton, 1992).

Our finding that most of the fiber stiffness seen during unloaded shortening appears to originate from weakly binding cross-bridges while only some 1–3% at most of all cross-bridges occupy strongly binding states leads to an interaction distance that is well within the range of the size of a cross-bridge, even for a large fraction of cross-bridges occupying strongly binding states during isometric contraction. With filament sliding of 1.6 (nm/h.s.)/s (at 5°C) and fiber ATPase during unloaded shortening of some 1.5 s^{-1}/myosin head (at 5°C; Brenner, 1988a,b; Houadjeto et al., 1991; Herrmann et al., 1993; Lionne et al., 1995), the interaction distance is ~20 nm and thus is not in contradiction with conventional cross-bridge models, i.e., with the concept that a cross-bridge can stay strongly attached at the same binding site on actin while passing through the strongly binding force-generating cross-bridge states. Thus there is no need for the additional assumption that strongly attached cross-bridges interact with several binding sites on actin to account for the maximum speed of shortening (e.g., Brenner 1991; Cooke et al., 1994; Piazzesi and Lombardi, 1995), although it is not ruled out that such reactions might occur to some extent. The estimate of the interaction distance on the basis of the work presented here is about an order of magnitude less than the values derived previously (Higuchi and Goldman, 1991, 1995; Burton, 1992). This difference is solely the result of our conclusion that most of the stiffness observed during unloaded shortening results from weak cross-bridge attachment to actin.

In the in vitro motility sliding assay, although the situation may be somewhat different from that in muscle fibers (H.E. Huxley, 1990; Burton, 1992), the interaction distance (here usually called the step size) of the cross-bridge has been derived from similar parameters, i.e., from the speed of filament sliding, the ATPase in the assay, and some estimate of the fraction of the cycling time during which a cross-bridge passes through strongly binding states (called the duty ratio). The duty ratio derived for in vitro motility assays is actually a model-dependent parameter. The values of the step size derived for in vitro motility assays vary between 5 and 200 nm, and it is the difference in the assumed duty ratio that is mainly responsible for this large range. The duty ratio favored by Spudich and co-workers (5%; Uyeda et al., 1990, 1991) is essentially identical to our estimate presented here; the duty ratio of Yanagida and co-workers (>50%; Harada and Yanagida, 1988; Harada et al., 1990; Saito et al., 1994) is much higher than our estimate of the duty ratio in fibers. The estimate of the duty ratio by Yanagida and co-workers is based on the assumption that only cross-bridges in strongly binding ("stroking") states can hold the actin filaments near the myosin-coated surface. However, it may well be possible that weakly attached cross-bridges may help to hold the actin filaments close to the surface by restricting Brownian motion, as suggested by Uyeda et al. (1991). These authors found that actin filaments can bind to the heavy meromyosin-coated surface of their assay in the presence of MgATPγS, an analog for weakly binding states. An estimate of the duty ratio by stochastic models neglecting such weak interactions (Harada and Yanagida, 1988; Harada et al., 1990; Saito et al., 1994) may therefore lead to an overestimate of the duty ratio and thus the step size.

Fraction of cross-bridges weakly attached during high-speed shortening

If only very few cross-bridges occupy strongly binding states during high-speed shortening, the fraction of cross-bridges weakly attached to actin at any one moment is essentially the same as expected for a pure population of weakly binding cross-bridges. From binding studies Stein and Chalovich (1991) determined that 54% of S1·ATP/S1·ADP·P_i is bound to regulated actin at low ionic strength (μ = 15 mM) and in the presence of Ca^{2+}. At their free actin concentration of 32 mM this results in an apparent binding constant of 1.7×10^4 M^{-1}. The binding constants of various S1 states for actin are known to decrease strongly when ionic strength is raised, essentially independently of the nucleotide (Greene et al., 1983). According to the results of Greene et al. (1983) the binding constant determined by Stein and Chalovich (1991) has to be corrected by a factor of 1/230 to account for the ionic strength used in our study (μ = 170 mM). Thus the binding constant of S1·ATP/S1·ADP·P_i for binding to actin would be 74 M^{-1}. Assuming that the factor to correlate binding of S1 to actin in solution with the binding of cross-bridges to actin in muscle (the "effective actin concentration") is the same in the presence of all nucleotides (1.5–5 mM; Brenner et al., 1986b), the binding constant of 74 M^{-1} from solution studies would translate into a binding constant for cross-bridges in the ATP/ADP·P_i states of 0.11–0.37. Thus, for our conditions the fraction of the weakly binding cross-bridges that are attached to actin at any one moment would be some 10–30%. This is consistent with the stiffness-speed relation derived for unloaded conditions (Fig. 7), considering that the majority of cross-bridges are in weakly binding states at a high speed of shortening and that only part of the stiffness-speed relation can be characterized experimentally.

Contribution of weakly binding cross-bridges to forces opposing high-speed shortening

According to the concept of A. F. Huxley (1957), the maximum speed of shortening is determined by a force balance between cross-bridges driving active shortening (positively strained) and cross-bridges opposing shortening (negatively strained). Usually it is assumed that only strongly attached cross-bridges oppose active shortening, i.e., that only strongly attached cross-bridges are relevant to the proposed force balance at v_{max}. With the possible contribution of weakly attached cross-bridges to fiber stiffness derived for unloaded shortening, even at moderate speeds of stretch, the question arises whether weakly attached cross-bridges can contribute to forces opposing filament sliding at high-speed shortening. If so, the average strain of strongly attached cross-bridges should not approach zero for unloaded conditions.

The average strain of attached cross-bridges might be derived from the y_o value, i.e., the release that must be applied per half-sarcomere to reduce the active force to zero. This value can be estimated from the ratio of generated force over stiffness contributed by strongly attached cross-bridges. Previously this ratio was derived for isometric and isotonic conditions, using total fiber stiffness (Fig. 10, *open symbols*), i.e., with the assumption that all fiber stiffness results from cross-bridges in strongly binding states. The plot of isotonic load/total observed stiffness (P/S) versus relative load approaches zero for unloaded shortening conditions. This is usually interpreted as a force equilibrium between positively and negatively strained strongly attached cross-bridges during unloaded shortening (cf. Julian and Sollins, 1975; Julian and Morgan, 1981; Ford et al., 1985; Griffiths et al., 1993). However, if not the total stiffness S but only the part estimated to originate from strongly attached cross-bridges is used to calculate the average strain of the strongly attached cross-bridges, a different behavior is seen (Fig. 10, *filled symbols*). It is worth noting that a possible contribution of filament compliance to fiber stiffness will not change this basic conclusion but only reduce the magnitude of the cross-bridge strain shown in Fig. 10. In this model, the remaining net strain of strongly attached cross-bridges at zero external load is balanced by negative forces originating from weak cross-bridge attachment. Such a possible effect of weak interactions on filament sliding was previously proposed by Tawada and Sekimoto (1991). These authors proposed that in vitro filament sliding velocity might be limited by weak cross-bridge interactions exerting a viscous-like drag. No experimental data, however, were available to estimate such a contribution or to determine whether it might also be relevant for limiting maximum unloaded shortening velocity in fibers. With our estimate of the occupancy of weakly versus strongly binding states at v_{max}, and with our estimate of the rate constants for reversible dissociation (k^-) of weakly attached cross-bridges from activated actin filaments during active unloaded shortening, we can evaluate a possible contribution of weakly attached cross-bridges to forces opposing shortening.

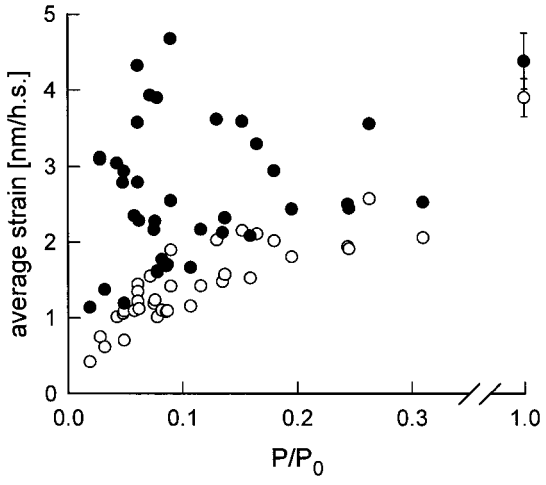

FIGURE 10 Average strain of strongly bound cross-bridges vesus load with and without contribution of weakly binding cross-bridges to isotonic stiffness. Data are derived from experiments performed at $T = -1°C$, μ = 170 mM, S.L. = 2.6 μm. Fiber stiffness was measured at a speed of stretch of 10^4 (nm/h.s.)/s. ○, Average strain of strongly bound cross-bridges calculated from the ratio P/S, where S is the total stiffness observed in the presence of the load P. This calculation is an estimate of y_0, for which any contribution of weakly bound cross-bridges to fiber stiffness is neglected. ●, Average strain of strongly bound cross-bridges based on the residual stiffness after the contribution of weakly bound cross-bridges is subtracted from the total observed stiffness. The average strain was calculated by $P/(S - S_w)$, where S_w is the fiber stiffness observed in the presence of MgATPγS under the same experimental conditions (same high Ca^{2+} concentration, passive shortening with similar velocities of filament sliding, similar sarcomere length).

Using the relation between k^-, v_{max}, and y_o as derived in the Appendix (Eq. 7), we can estimate, as an extreme, how slowly weakly attached cross-bridges have to detach to generate all of the forces opposing filament sliding at v_{max}. With average estimates of the fraction of strongly and weakly attached cross-bridges (2% resp. 20%) at v_{max} (700 (nm/h.s.)/s) and the isometric value for y_0 (y_0^{isom} = 4 nm/h.s.), dissociation of weakly attached cross-bridges has to be $2 \times 10^3\ s^{-1}$ (values are derived from experiments at −1°C). This is still about a factor of 5 slower than we estimated from stiffness-speed relations ($\geq 10^4\ s^{-1}$). Thus, from this calculation we expect that weakly bound cross-bridges could balance ~20% of the force generated by strongly bound cross-bridges. However, at 5°C with the higher v_{max} (1.600 (nm/h.s.)/s; y_0^{isom} = 5.6 nm/h.s.), the calculated value for k^- ($4 \times 10^3\ s^{-1}$) becomes closer to the values of k^- derived from stiffness-speed relations, which are still $\sim 10^4\ s^{-1}$, because stiffness-speed relations seem not to be affected over this temperature range (see Fig. 9 *B*). These calculations reveal two viewpoints: on the one hand, weakly bound cross-bridges may well contribute significantly to forces opposing filament sliding, the extent of which de-

pends on the experimental conditions. This makes it possible that weakly attached cross-bridges may be one of the factors that limit shortening velocity near v_{max}, as was previously suggested by Tawada and Sekimoto (1991). On the other hand, the amount of negative force built up by weakly attached cross-bridges does not exceed the amount of positive force generated by strongly attached cross-bridges during high-speed shortening. Thus a high ratio of weakly to strongly attached cross-bridges does not give rise to too high counteractive forces exerted by weakly bound cross-bridges.

How much of the mechanical energy generated by force-generating cross-bridges will be consumed by such passively strained weakly attached cross-bridges at v_{max}? Calculating the ratio E_W/E_S of mechanical energy stored in weakly to strongly attached heads according to Eq. 8 derived in the Appendix, using the values for 5°C (v_{max} = 1.600 (nm/h.s.)/s, y_0^{isom} = 5.6 nm/h.s., $k^- = 4 \times 10^3\ s^{-1}$) yields a value of −0.15. This means that even if weakly attached cross-bridges would carry the whole component of negative force at v_{max}, this would consume only a little (15%) of the mechanical energy provided by force-generating cross-bridges. This reveals that during high-speed shortening even a fraction of weakly attached cross-bridges that is much larger than the fraction of strongly attached cross-bridges would not reduce the efficiency of chemomechanical energy coupling by much.

CONCLUDING REMARKS

The most important result found in this study is that stiffness-speed relations for high-speed isotonic contraction are distinctly different from those observed during isometric contraction or during relaxation. The isotonic stiffness-speed relation, however, is essentially identical to that seen in activated fibers in the presence of MgATPγS, i.e., under conditions where all cross-bridges occupy weakly binding states but interact with activated thin filaments. These results support the idea that the majority of cross-bridges attached to actin during shortening at v_{max} are fast detaching weakly bound cross-bridges, and the calculations carried out here confirm that this idea does not lead to thermodynamic inconsistencies. Our findings once more illustrate that a decreased fiber stiffness observed under just a single speed of stretch (or single frequency of sinusoidal oscillation) can easily be misinterpreted when taken as direct measure of changes in strong cross-bridge attachment. Only measuring stiffness over a sufficient range of speed of stretch (or oscillation frequencies) can detect a possible contribution of weakly attached cross-bridges to fiber stiffness. In the present study the changes in speed dependence of stiffness that occur with the change from isometric contraction to unloaded shortening appear to reflect an almost complete redistribution from strongly binding to weakly binding states. The functional relevance of the weakly attached cross-bridges during high-speed shortening is still unclear. Aside from being a precursor of force-generating states, weak cross-bridge attachment may take a role in dynamically guarding thin filaments during their sliding motion and in stabilizing the interfilament arrangement during high-speed shortening.

APPENDIX

To discuss the extreme, we estimate how slowly weakly binding cross-bridges have to detach during unloaded shortening to carry *all* of the negative force, i.e., that weakly bound cross-bridges will generate all of the negative force, whereas strongly bound cross-bridges generate the positive force.

Let N_W and N_S be, respectively, the fraction of weakly and strongly bound cross-bridges during shortening at v_{max}. For a first approximation, we assume all strongly bound cross-bridges strictly generating force to be homogeneously distributed at different strains (x) between 0 and D_W, which we refer to (Burton, 1992) as the working stroke per attachment of a strongly bound cross-bridge. This can be defined in the form of a distribution function $N_S(x)$ describing the occupancy of strongly bound cross-bridges as a function of strain with the following properties:

$$N_S = \int_{x=-\infty}^{\infty} N_S(x)\mathrm{d}x,$$

$$\text{where } N_S(x) = \begin{cases} N_S^0 & \text{for } 0 \le x \le D_W \\ 0 & \text{for } x < 0;\ x > D_W \end{cases} \quad (1)$$

Solving the integral over the range of relevant strain, one obtains

$$N_S = \int_{x=0}^{D_W} N_S(x)\mathrm{d}x \Rightarrow N_S^0 = \frac{N_S}{D_W} \quad (2)$$

We assume that the working stroke is independent of load. However, this is a simplification, but it follows from our limiting case that strongly bound cross-bridges will strictly generate force. At any load the average strain of strongly bound cross-bridges will therefore be ½ D_W. The most reliable method of estimating this value is to take the y_0 value determined at isometric contraction at which the contribution of weakly bound cross-bridges to fiber stiffness becomes small:

$$y_0^{isom} \approx \tfrac{1}{2} \cdot D_W \quad (3)$$

We assume further that cross-bridges of the weakly binding type attach in a distribution symmetrical to $x = 0$ and that detachment of all weakly bound cross-bridges can be described by a first-order reaction with a single rate constant k^-. The filament sliding will then produce a shift in the distribution of weakly bound cross-bridges toward the region of negative force according to

$$N_W = \int_{x=-\infty}^{\infty} N_W(x)\mathrm{d}x,$$

$$\text{where } N_W(x) = \begin{cases} N_W^0 \cdot \exp([k^-/v_{max}] \cdot x) & \text{for } x \le 0 \\ 0 & \text{for } x > 0 \end{cases} \quad (4)$$

$$N_W = \int_{x=-\infty}^{0} N_W(x)dx \Rightarrow N_W^0 = \frac{N_W \cdot k^-}{v_{max}} \quad (5)$$

Let S_W and S_S be the strain-independent stiffness of the fraction of cross-bridges occupying weakly attached and strongly attached states, respectively. The relationship for the force balance is then

$$\int_{x=0}^{D_W} S_S \cdot x \cdot N_S(x)dx + \int_{x=-\infty}^{0} S_W \cdot x \cdot N_W(x)dx = 0 \quad (6)$$

Inserting the distribution functions from Eqs. 1 and 4, replacing N_S^0 and N_W^0 by the use of Eqs. 2 and 5, solving the integrals, and replacing D_W according to Eq. 3 results in a simple relationship, containing only parameters that can be derived from observable quantities:

$$S_S \cdot N_S \cdot y_0^{isom} \approx S_W \cdot N_W \cdot \frac{v_{max}}{k^-} \quad (7)$$

If we solve double integrals instead of single integrals of the terms in Eq. 6, we obtain, respectively, the elastic energy of strongly attached cross-bridges (E_S) and that of weakly attached cross-bridges (E_W) supporting filament sliding:

$$E_S \approx \frac{2}{3} \cdot S_S \cdot N_S \cdot (y_0^{isom})^2$$

$$\text{and} \quad E_W = -2 \cdot S_W \cdot N_W \cdot \left(\frac{v_{max}}{k^-}\right)^2 \quad (8)$$

REFERENCES

Adelstein, R. S., and E. Eisenberg. 1980. Regulation and kinetics of the actin-myosin-ATP interaction. *Annu. Rev. Biochem.* 49:921–956.

Bagshaw, C. R., J. F. Eccleston, F. Eckstein, R. S. Goody, H. Gutfreund, and D. R. Trentham. 1974. The magnesium-ion dependent adenosine triphosphatase of myosin. *Biochem. J.* 141:331–349.

Bagshaw, C. R., J. F. Eccleston, D. R. Trentham, D. W. Yates, and R. S. Goody. 1972. Transient kinetic studies of the Mg^{2+}-dependent ATPase of myosin and its proteolytic subfragments. *Cold Spring Harb. Symp. Quant. Biol.* 37:127–135.

Brenner, B. 1980. Effect of free sarcoplasmic Ca^{2+} concentration on maximum unloaded shortening velocity: measurements on single glycerinated rabbit psoas fibers. *J. Muscle Res. Cell Motil.* 1:409–428.

Brenner, B. 1983a. Technique for stabilizing the striation pattern in maximally calcium-activated skinned rabbit psoas fibers. *Biophys. J.* 41: 99–102.

Brenner, B. 1983b. Cross-bridge attachment during isotonic shortening in single skinned rabbit psoas fibers. *Biophys. J.* 41:33a.

Brenner, B. 1985. Sarcomeric domain organization within single skinned rabbit psoas fibers and its effects on laser light diffraction patterns. *Biophys. J.* 48:967–982.

Brenner, B. 1986. The cross-bridge cycle in muscle. Mechanical, biochemical, and structural studies on single skinned rabbit psoas fibers to characterize cross-bridge kinetics in muscle for correlation with the actomyosin-ATPase in solution. *Basic Res. Cardiol.* 81:1–15.

Brenner, B. 1988a. An experimental approach to determine cross-bridge turnover kinetics during isometric and isotonic steady-state contraction using skinned skeletal muscles of the rabbit. *Pflügers Arch.* 411(Suppl. 1):R186.

Brenner, B. 1988b. Effect of Ca^{2+} on cross-bridge turnover kinetics in skinned single rabbit psoas fibers: implications for regulation of muscle contraction. *Proc. Natl. Acad. Sci. USA.* 85:3265–3269.

Brenner, B. 1990. Muscle mechanics and biochemical kinetics. *In* Molecular Mechanisms in Muscular Contraction. Topics in Molecular and Structural Biology, Vol. 13. J. M. Squire, editor. Macmillan Press, Houndmills, UK. 77–149.

Brenner, B. 1991. Rapid dissociation and reassociation of actomyosin cross-bridges during force generation: a newly observed facet of cross-bridge action in muscle. *Proc. Natl. Acad. Sci. USA.* 88:10490–10494.

Brenner, B. 1993. Further analysis of cross-bridge turnover kinetics during isotonic contraction in skinned rabbit psoas fibers. *Biophys. J.* 64:345a.

Brenner, B. 1998. Muscle mechanics II: skinned muscle fibres. *In* Current Methods in Muscle Physiology. H. Sugi, editor. Oxford University Press, Oxford, UK. 33–69.

Brenner, B., J. M. Chalovich, L. E. Greene, E. Eisenberg, and M. Schoenberg. 1986a. Stiffness of skinned rabbit psoas fibers in MgATP and PP_i solution. *Biophys. J.* 50:685–691.

Brenner, B., and R. Stehle. 1994. Cross-bridge cycling kinetics during isotonic contraction of skinned rabbit psoas fibers. *J. Muscle Res. Cell Motil.* 15:202. (abstract).

Brenner, B., L. C. Yu, L. E. Greene, E. Eisenberg, and M. Schoenberg. 1986b. Ca^{2+}-sensitive cross-bridge dissociation in the presence of magnesium pyrophosphate in skinned rabbit psoas fibers. *Biophys. J.* 50: 1101–1108.

Burton, K. 1992. Myosin step size: estimates from motility assays and shortening muscle. *J. Muscle Res. Cell. Motil.* 13:590–607.

Chase, P. B., and M. J. Kushmerick. 1988. Effect of pH on contraction of rabbit fast and slow skeletal muscle fibers. *Biophys. J.* 53:935–946.

Cooke, R., M. S. Crowder, and D. D. Thomas. 1982. Orientation of spin labels attached to cross-bridges in contracting muscle fibers. *Nature.* 300:776–778.

Cooke, R., H. White, and E. Pate. 1994. A model of the release of myosin heads from actin in rapidly contracting muscle fibers. *Biophys. J.* 66: 778–788.

Eisenberg, E., and L. E. Greene. 1980. The relation of muscle biochemistry to muscle physiology. *Annu. Rev. Physiol.* 42:293–309.

Eisenberg, E., and T. L. Hill. 1978. A cross-bridge model of muscle contraction. *Prog. Biophys. Mol. Biol.* 33:55–82.

Eisenberg, E., and T. L. Hill. 1985. Muscular contraction and free energy transduction in biological systems. *Science.* 227:999–1006.

Eisenberg, E., T. L. Hill, and Y. Chen. 1980. Cross-bridge model of muscle contraction. Quantitative analysis. *Biophys. J.* 29:195–227.

Ford, L. E., A. F. Huxley, and R. M. Simmons. 1985. Tension transients during steady shortening of frog muscle fibers. *J. Physiol. (Lond.).* 361:131–150.

Goldman, Y. E., and R. M. Simmons. 1977. Active and muscle rigor stiffness. *J. Physiol. (Lond.).* 269:55–57.

Goody, R. S., and W. Hofmann. 1980. Stereochemical aspects of the interaction of myosin and actomyosin with nucleotides. *J. Muscle Res. Cell Motil.* 1:101–115.

Greene, L. E., J. R. Sellers, E. Eisenberg, and R. S. Adelstein. 1983. Binding of gizzard smooth muscle myosin subfragment 1 to actin in the presence and absence of adenosine 5′-triphosphate. *Biochemistry.* 22: 530–535.

Griffiths, P. J., C. C. Ashley, M. A. Bani, Y. Maéda, and G. Cecchi. 1993. Cross-bridge attachment and stiffness during isotonic shortening of intact single muscle fibers. *Biophys. J.* 64:1150–1160.

Harada, Y., K. Sakurada, T. Aoki, D. D. Thomas, and T. Yanagida. 1990. Mechanochemical coupling in actomyosin energy transduction studied by in vitro motility assay. *J. Mol. Biol.* 216:49–68.

Harada, Y., and T. Yanagida. 1988. Direct observation of molecular motility by light microscopy. *Cell Motil. Cytoskel.* 10:71–76.

Haugen, P. 1986. The stiffness under isotonic releases during a twitch of a frog muscle fiber. *Adv. Exp. Med. Biol.* 226:461–469.

Herrmann, C., J. Sleep, P. Chaussepied, F. Travers, and T. Barman. 1993. A structural and kinetic study on myofibrils prevented from shortening by chemical cross-linking. *Biochemistry.* 32:7255–7263.

Higuchi, H., and Y. E. Goldman. 1991. Sliding distance between actin and myosin filaments per ATP molecule hydrolyzed in skinned muscle fibers. *Nature.* 352:352–354.

Higuchi, H., and Y. E. Goldman. 1995. Sliding distance per ATP molecule hydrolyzed by myosin heads during isotonic shortening of skinned muscle fibers. *Biophys. J.* 69:1491–1507.

Higuchi, H., T. Yanagida, and Y. E. Goldman. 1995. Compliance in thin filaments in skinned fibers of rabbit skeletal muscle. *Biophys. J.* 69: 1000–1010.

Hill, T. L. 1974. Theoretical formalism for the sliding filament model of contraction of striated muscle. Part I. *Prog. Biophys. Mol. Biol.* 28: 267–340.

Houadjeto, M., T. Barman, and F. Travers. 1991. What is the true ATPase activity of contracting myofibrils. *FEBS Lett.* 281:105–107.

Huxley, A. F. 1957. Muscle structure and theories of contraction. *Prog. Biophys. Biophys. Chem.* 7:255–318.

Huxley, A. F., and R. M. Simmons. 1971. Proposed mechanism of force generation in striated muscle. *Nature.* 233:533–538.

Huxley, A. F., and R. M. Simmons. 1973. Mechanical transients and the origin of molecular force. *Cold Spring Harb. Symp. Quant. Biol.* 37: 669–680.

Huxley, H. E. 1969. The mechanism of muscular contraction. *Science.* 164:1356–1366.

Huxley, H. E. 1990. Sliding filaments and molecular motile systems. *J. Biol. Chem.* 265:8347–8350.

Huxley, H. E., A. Stewart, H. Sosa, and T. Irving. 1994. X-ray diffraction measurements of the extensibility of actin and myosin filaments in contracting muscle. *Biophys. J.* 67:2411–2421.

Julian, F. J., and D. L. Morgan. 1981. Variation of muscle stiffness with tension during tension transients and constant velocity shortening in the frog. *J. Physiol. (Lond.).* 319:193–203.

Julian, F. J., and M. R. Sollins. 1975. Variation of muscle stiffness with force at increasing speeds of shortening. *J. Gen. Physiol.* 66:287–302.

Kojima, H., A. Ishijima, and T. Yanagida. 1994. Direct measurement of stiffness of single actin filaments with and without tropomyosin by in vitro nanomanipulation. *Proc. Natl. Acad. Sci. USA.* 91:12962–12966.

Kraft, T., L. C. Yu, H. J. Kuhn, and B. Brenner. 1992. Effect of Ca^{2+} on weak cross-bridge interaction with actin in the presence of adenosine 5′-[γ-thio]triphosphate. *Proc. Natl. Acad. Sci. USA.* 89:11362–11366.

Linari, M., I. Dobbi, M. Reconditi, N. Koubassova, M. Irving, G. Piazzesi, and V. Lombardi. 1998. The stiffness of skeletal muscle in isometric contraction and rigor: the fraction of myosin heads bound to actin. *Biophys. J.* 74:2459–2473.

Lionne, C., M. Brune, M. R. Webb, F. Travers, and T. Barman. 1995. Time resolved measurements show that phosphate release is the rate limiting step on myofibrillar ATPases. *FEBS Lett.* 164:59–62.

Lombardi, V., G. Piazzesi, and M. Linari. 1992. Rapid regeneration of the actin-myosin power stroke in contracting muscle. *Nature.* 355:638–641.

Lymn, R. W., and E. W. Taylor. 1971. Mechanism of adenosine triphosphate hydrolysis by actomyosin. *Biochemistry.* 10:4617–4624.

Ma, Y-Z., and E. W. Taylor. 1994. Kinetic mechanism of myofibril ATPase. *Biophys. J.* 66:1542–1553.

Ostap, E. M., V. A. Barnett, and D. D. Thomas. 1995. Resolution of three structural states of spin-labeled myosin in contracting muscle. *Biophys. J.* 69:177–188.

Pate, E., H. White, and R. Cooke. 1993. Determination of the myosin step size from mechanical and kinetic data. *Proc. Natl. Acad. Sci. USA.* 90:2451–2455.

Piazzesi, G., F. Francini, M. Linari, and V. Lombardi. 1992. Tension transients during steady lengthening of tetanized muscle fibers from the frog. *J. Physiol. (Lond.).* 445:659–711.

Piazzesi, G., and V. Lombardi. 1995. A cross-bridge model that is able to explain mechanical and energetical properties of a shortening muscle. *Biophys. J.* 68:1966–1979.

Rayment, I., H. M. Holden, M. Whittaker, C. B. Yohn, M. Lorenz, K. C. Holmes, and R. A. Milligan. 1993. Structure of the actomyosin complex and its implications for muscle contraction. *Science.* 261:58–65.

Rosenfeld, S. S., and E. W. Taylor. 1984. The mechanism of regulation of actomyosin subfragment 1 ATPase. *J. Biol. Chem.* 262:9984–9993.

Rüdel, R., and F. Zite-Ferenczi. 1979. Interpretation of light diffraction by cross-striated muscle as Bragg reflexion of light by the lattice of contractile proteins. *J. Physiol. (Lond.).* 290:317–330.

Sabido-David, C., S. C. Hopkins, L. D. Saraswat, S. Lowey, Y. E. Goldman, and M. Irving. 1998. Orientation changes of fluorescent probes at five sites on the myosin regulatory light chain during contraction of single skeletal muscle fibers. *J. Mol. Biol.* 279:387–402.

Saito, K., Ta. Aoki, To. Aoki, and T. Yanagida. 1994. Movement of single myosin filaments and myosin step size on an actin filament suspended in solution by a laser trap. *Biophys. J.* 66:769–777.

Schoenberg, M. 1985. Equilibrium muscle cross-bridge behavior. Theoretical considerations. *Biophys. J.* 48:467–475.

Schoenberg, M. 1988. Characterization of the myosin adenosine triphosphate (M.ATP) cross-bridge in rabbit and frog skeletal muscle fibers. *Biophys. J.* 54:135–148.

Schoenberg, M., B. Brenner, J. M. Chalovich, L. E. Greene, and E. Eisenberg. 1984. Cross-bridge attachment in relaxed muscle. *Adv. Exp. Med. Biol.* 170:269–284.

Siemanowsky, R. F., M. O. Wiseman, and H. D. White. 1985. ADP dissociation from actomyosin subfragment 1 is sufficiently slow to limit the unloaded shortening velocity in vertebrate muscle. *Proc. Natl. Acad. Sci. USA.* 82:658–662.

Stehle, R., and B. Brenner. 1994. Characterization of cross-bridge states during high-speed shortening. Effect of inorganic phosphate (P_i) and temperature (T). *Biophys. J.* 66:191a.

Stehle, R., T. Kraft, and B. Brenner. 1993. Stiffness-speed relations for isometric and isotonic contraction. Significance for occupancy of strong-binding states during high-speed shortening. *Biophys. J.* 64:250a.

Stein, L. A., and J. M. Chalovich. 1991. Activation of skeletal S-1 ATPase activity by actin-tropomyosin-troponin. *Biophys. J.* 60:399–407.

Tawada, K., and K. Sekimoto. 1991. A physical model of ATP-induced actin myosin movement in vitro. *Biophys. J.* 59:343–356.

Uyeda, T. Q. P., S. J. Kron, and J. A. Spudich. 1990. Myosin step size. Estimation from slow sliding movement of actin over low densities of heavy meromyosin. *J. Mol. Biol.* 214:699–710.

Uyeda, T. Q. P., H. M. Warrick, S. J. Kron, and J. A. Spudich. 1991. Quantized velocities at low myosin densities in an in vitro motility assay. *Nature.* 352:307–311.

Wakabayashi, K., Y. Sugimoto, H. Tanaka, Y. Ueno, Y. Takezawa, and Y. Amemiya. 1994. X-ray diffraction evidence for the extensibility of actin and myosin filaments during muscle contraction. *Biophys. J.* 67: 2422–2435.

Yu, L. C., and B. Brenner. 1989. Structures of actomyosin cross-bridges in relaxed and rigor muscle fibers. *Biophys. J.* 55:441–453.